Journal Name

Dynamic Article Links ►

Cite this: DOI: 10.1039/c0xx00000x

www.rsc.org/xxxxxx

ARTICLE TYPE

Using Gel Morphology to Control Pore Shape

Jonathan A. Foster,*[a] David W. Johnson,[a] Mark-Oliver M. Pipenbrock[a] and Jonathan W. Steed*[a]

Received (in XXX, XXX) Xth XXXXXXXXX 20XX, Accepted Xth XXXXXXXXX 20XX
DOI: 10.1039/b000000x

Supramolecular gelators with different fibre morphologies have been used as templates to form mesoporous covalent polymers with different pore shapes. Two bis-urea derived gelators functionalised with different amino-acid groups form gels in 1:1 methyl methacrylate : ethylene glycol dimethacrylate (MMA:EGDMA) mixtures with either ribbon-like or cylindrical fibre morphologies. Polymerisation of the monomer produces composite materials containing the gelators. The gel template can be readily removed by washing with methanol to give porous materials in which the gel morphology is imprinted on the covalent polymer matrix. Scanning electron microscopy measurements show the resulting polymers exhibit strikingly different pore shapes corresponding to those expected for the differently shaped gel fibres. Nitrogen adsorption measurements corroborate these observations showing mesoporous materials with considerable BET surface areas, adsorption-desorption isotherms, and pore size profiles. Gelator concentration provides a ready means of controlling porosity and samples prepared at different gelator concentrations are compared. Small changes in the molecular structure of the gelator can therefore be used to produce polymeric materials with very different pore shapes, sizes and adsorption characteristics.

Introduction

A variety of low molecular weight gelators (LMWGs) have been found to self-assemble into supramolecular structures capable of immobilising solvent to form a gel.[1-3] These gels adopt a number of nanoscopic morphologies including fibrous, helical, ribbon-like, tubular, lamellar and vesicular structures.[4-6] As well as finding applications in their own right[3, 7, 8] such frameworks have been used as scaffolds to template the formation of rigid, nanostructured materials. The soft structure of the gels can be 'fixed' in a variety of ways, for example by depositing an inorganic material on the inner or outer surface of the template, or by using LMWGs which can themselves be polymerised to give a rigid structure.[4, 9-11] LMWGs able to gel polymer precursors such as styrene or methyl methacrylate which can subsequently be polymerised have also been used to give composite materials.[12, 13] Such composites may show enhanced mechanical,[14, 15] fluorescence[13, 16] or optical[17] properties compare to those of the pure polymer. The supramolecular nature of the gel matrix means it can be easily removed by washing or chemical treatment of the composites to leave an imprint of the gel structure in the polymer.[12, 18-21] A number of fibrillar,[19, 22, 23] helical,[21, 24] tubular and macro-porous structures[25] have been imprinted in this way giving rise to porous materials with different pore size, shape and connectivity profiles. Such mesoporous materials have found use in applications such as filtration, storage, catalysis, cell growth, drug delivery and as rewritable materials.[13, 21, 26-29]

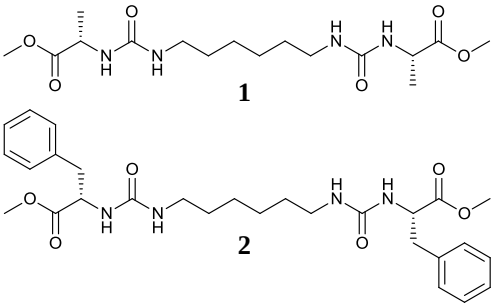

1

2

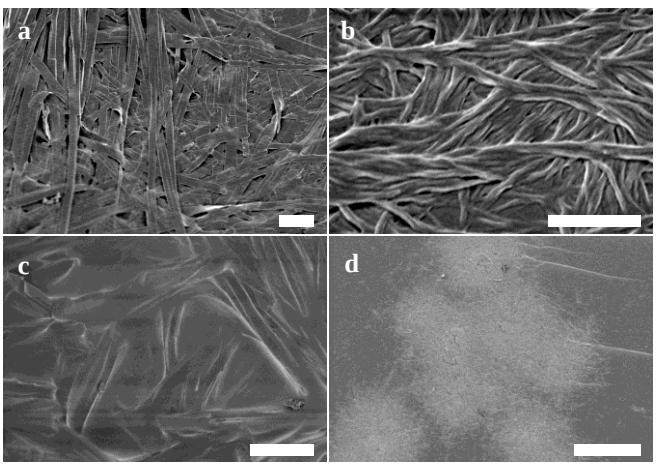

Figure 1 SEM images showing a) 5 % w/v xerogel of **1** [1 μm] b) 2 % w/v xerogel of **2** [500 nm] c) unwashed composite of 10 % w/v **1** in 1:1 MMA:EGDMA [5 μm] d) unwashed composite of 5 % w/v **2** in 1:1 MMA:EGDMA [5 μm] with distance denoted by white scale bar given in square brackets

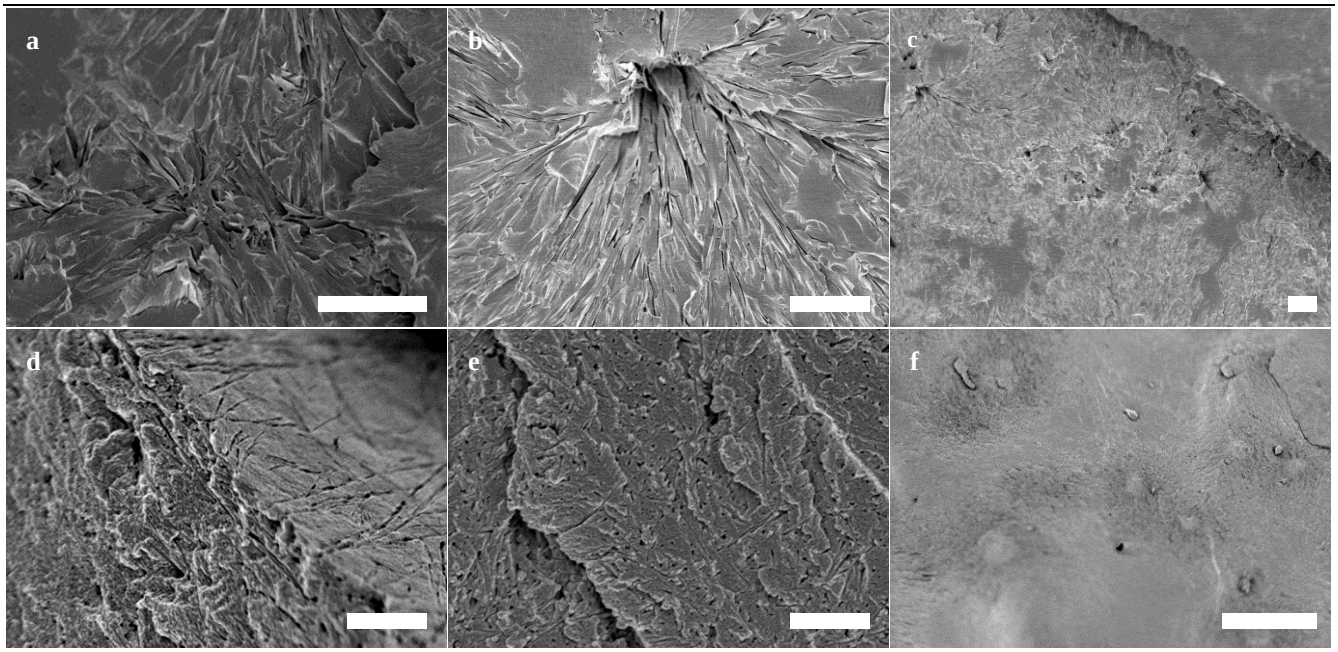

Figure 2 SEM images showing the different pore morphologies resulting from the imprinting of different concentrations of gelator: a) 1 % w/v **1** [5 μm] b) 5 % w/v **1** [5 μm] c) 10 % w/v **1** [10 μm], d) 5 % w/v **2** [500 nm] e) 5 % w/v **2** [500 nm] f) 10 % w/v **2** [20 μm] with distance denoted by white scale bar given in square brackets

The present study utilises two hexylene spaced bis-urea gelators functionalised with either alanine or phenylalanine derived end groups, namely **1** and **2** respectively (Scheme 1).[30, 31] The compounds gel a variety of solvents including a 1:1 mixture of polymer precursor methyl methacrylate (MMA) and cross-linker ethylene glycol dimethacrylate (EGDMA). Electron microscopy revealed that the mesoscopic morphology of the gels is different for the two compounds with xerogels of **2** showing small cylindrical fibres whilst **1** consists of two-dimensional ribbon-like structures (Figure 1). It was envisioned that polymerisation of the MMA:EGDMA solvent and subsequent washing with methanol to remove the gelator would produce meso-porous polymers with pore structures mirroring those of the templates.

Results and discussion

The gels are formed by heating a set amount of gelator **1** or **2** (0, 1, 2, 5, 10 or 20 % weight/volume) in 1 ml of 1:1 MMA:EGDMA (volume/volume) in a sealed vial using a heat-gun to give a clear solution. A high concentration of cross-linker was chosen to minimise rearrangement upon washing.[19] Gelation occurs rapidly upon cooling to room temperature. Polymers may be prepared using 1,1′-azobis(cyclohexane carbonitrile)[32] as a polymerisation initiator. This initiator is thermally sensitive so was allowed to diffuse into the gel for 18 h from a concentrated solution layered on top of the preformed gels. Alternatively, a blend of diphenyl (2, 4, 6-trimethylbenzyl)phosphine oxide and 2-hydroxy-2-methylpropiophenone can be used as the initiator which is thermally stable so able to be heated along with the gelator ensuring a more even distribution.

Polymerisation was induced by irradiating the samples with UV light (254 nm) for 24 hours. The gelator was then removed by washing the samples with hot methanol in a Soxhlet apparatus for up to three days. Removal of the gelator was confirmed by both chemical analysis which showed no nitrogen in the washed samples from either gelator or initiator, and by NMR spectroscopy of extracts from polymer samples immersed in DMSO-d_6 for several hours which showed no signals corresponding to gelator. Polymer samples were dried under vacuum to remove residual methanol.

SEM images of xerogels of **1** formed from the un-polymerised 1:1 MMA:EGDMA gel revealed two-dimensional ribbon-like structures (Figure 1a). The ribbons have a consistent thickness of ~25 nm, but exhibit considerable variation in width ranging from hundreds of nanometres to several micrometres. In contrast, SEM images of **2** prepared in the same way indicate a tangled network of one-dimensional fibrous strands (Figure 1b). The diameter of individual fibres is relatively uniform (~50 nm) though they are often tangled together into larger bunches. A helical twist reflecting the chirality of the gelator is evident in some fibres indicating they may be composed of smaller fibrils twisted together as a result of differing surface energies.[33-35] Increasing the concentration of gelator has little effect on the dimensions of the fibres. The difference in morphology between the two gelators is thought to be due to differences in the underlying packing of the molecules in the gel fibres.

Following polymerisation, evidence of the presence of the gel fibres within the polymerised sample could be seen in the unwashed gel-polymer composites, for example in the case of **1** where ribbons protruding from, and running along the surface of the polymer can be clearly seen (Figure 1c). Some contraction of the polymer or gelator appears to have taken place with gaps between the gel ribbons and surrounding polymers evident. Less obvious traces of the fibres of **2** were observed in the composites, possibly due to their smaller size making them difficult to distinguish from the polymer surface (Figure 1d).

Washing the polymerised gels with methanol to remove the gelator produced polymers with a variety of features consistent with the imprinting of gel fibres. Gelator **1** left slits and ribbon-like

Table 1 Summary of nitrogen gas adsorption data for washed polymers templated with various concentrations of compounds **1** and **2**

	Composition of gelator template					
Gelator	**1**			**2**		
Concentration	1 % w/v	5 % w/v	10 % w/v	1 % w/v	5 % w/v	10 % w/v
Skeletal density (g/cm^3)	1.2675 ±0.0019	1.2816 ±0.0067	1.2605 ±0.0011	1.2695 ±0.0019	1.2233 ±0.0020	1.2458 ±0.0019
BET Surface Area (m^2/g)	0.5425 ± 0.0074	0.2487 ± 0.0099	4.818 ± 0.027	1.209 ±0.011	12.974 ±0.049	29.70 ±0.14
BET constant, *C*	66.58	31.32	80.87	70.01	87.97	97.94
Correlation Coefficient	0.9992	0.9935	0.9998	0.9996	0.9999	0.9999
BJH average pore diameter (nm)	17.10	36.03	22.94	8.66	8.71	8.84

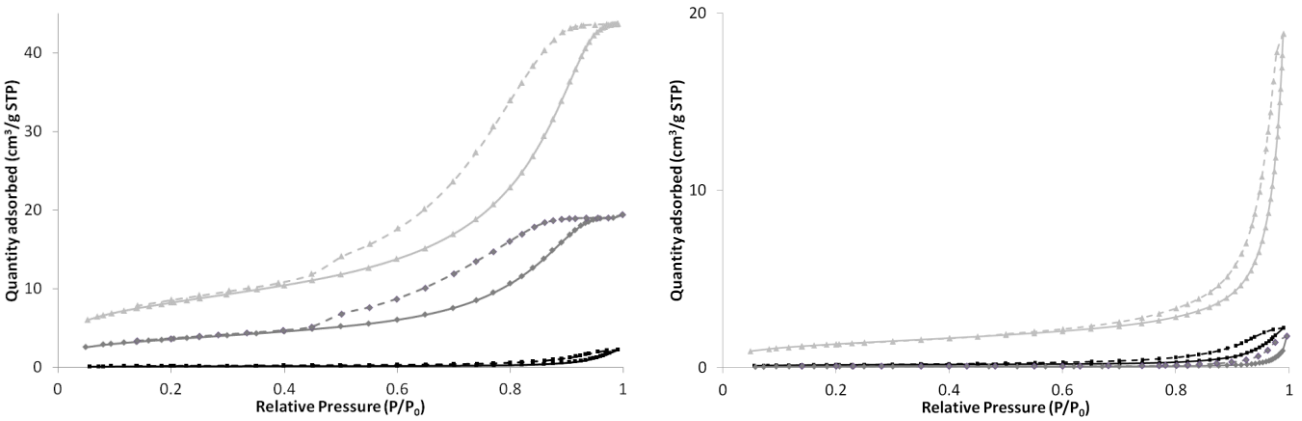

Figure 3 BET isotherm showing adsorption (solid) and desorption (dashed) isotherms for washed polymer samples formed by 1 % w/v (black), 5 % w/v (grey), 10 % w/v (light grey) of gelators **1** (a) and **2** (b)

grooves in the polymer surface with dimensions consistent with those seen for the xerogels (Figure 2a-c). These features tend to be in isolated patches at lower concentrations whilst at high concentrations less well defined, macro-porous materials are formed. Polymers formed by **2** showed fibre-like imprints and cylindrical pores (Figure 2d-f), again consistent with the gel morphology. The shape of individual pores tends to be poorly defined, presumably due to bunching of fibres and differences in the angle at which the fibre intersects the surface.

Interestingly, for polymers formed by both **1** and **2** the porous features are not evenly distributed throughout the sample (see Figure 2c and f) but tend to be bunched together, separated by patches of smooth polymer. In some cases the direction of the fibres appears to have been aligned. This presumably reflects bunching and entanglement of the fibres in the gel phase. This inhomogeneity and aligning is often seen in SEM images of collapsed xerogels and their presence in the polymers indicates that this is a real property of the gels rather than a result of the drying process. It is possible that this bunching may arise from partial phase separation between polymer and gel fibres.

In general the polymers proved relatively inhomogeneous with different fragments displaying a variety of different surface textures, some of which contain no evidence of imprinting (see supplementary information for further images). It is thought that the smooth fragments represent portions of the polymer resting against the glass sides of the vial or at the gel surface, as observed by optical microscopy in Figure S7. 1:1 PMMA:EGDMA reference samples, formed using the same processes but without gelator, showed a number of different textured surfaces and occasional holes (Figure S8). However, none of the features described for any of the imprinted polymers were observed in the reference samples.

Nitrogen adsorption-desorption isotherms of samples of polymers with 1, 5 and 10 % w/v **1** or **2** confirmed the formation of mesoporous structures by both gelators. Results are summarised in Table 1 and the isotherms are shown in Figure 3. Densities, as measured by gas pycnometry were found to be approximately constant across all samples ranging between 1.22-1.28 g cm^{-3}. No correlation between density and concentration of gelator was observed, indicating an open pore structure in all cases.

BET surface area measurements show the polymers produced by **1** have substantially lower surface areas (0.2-4.8 m^{2}g^{-1}) than those templated by **2** (1.2-30.0 m^{2}g^{-1}). It is worth noting that whilst the absolute surface areas for both polymer types are low compared to materials such as charcoal (400 m^{2}g^{-1})[36] or zeolites (50-1250 m^{2}g^{-1}),[37] this is unsurprising given the low porosity of the materials (<10%) and the presence of macroporosity as indicated by SEM. The surface areas are high when compared with other types of templated polymer which exhibit only macroporosity such as polyHIPEs (3 m^{2}g^{-1}, 79% nominal porosity) indicating a predominantly mesoporous structure.[38] The surface areas increase with the concentration of **2** as expected. The trend is less clear for polymers of **1** with the 5 % w/v sample showing an unexpectedly low surface area compared to the other samples.

Gas adsorption isotherms have been IUPAC classified based on empirical observations about the shape of isotherms and hysteresis loops obtained from different materials.[39] Both series of materials show type IV isotherms with the characteristic hysteresis loops associated with mesopores. The hysteresis loop shape matches that of an Type IV H2 isotherm which is characteristic of relatively disordered porous material.[39] The sudden increase in the gradient of the desorption curve at relative pressures of 0.4-0.5 is attributed to the phenomena of forced closing and indicates channels of

varying diameter. Other 'kinks' in the curves are thought to represent inhomogeneity either in the surface chemistry or pore structure

In polymers templated by **1** a plateau is rapidly reached at low pressures associated with completion of the nitrogen monolayer adsorption (Figure 3a). This is followed by the unrestricted adsorption of nitrogen at higher pressures with no saturation occurring. The hysteresis loop shape matches that of a type IV H3 isotherm which is characteristic of materials with narrow, slit-like pores such as those which are observed when plate-like materials agglomerate.[39] No forced closing is seen at 0.4-0.45 relative pressure which indicates a relatively uniform pore diameter.

The average pore diameters for the templated polymers, calculated using the BJH model,[40] are given in Table 1 and the pore size distribution is shown in figures S10 and S11. The data for the **2** series is calculated from the adsorption curves to avoid complications due to forced closing in the desorption isotherms.[40] The average pore diameter is 8-9 nm in polymers templated with **2** and there is a narrow distribution of pore sizes centred on the average (Figure S10). The pore volume increases with the concentration of gelator and the range of pore diameters increases from an upper limit of 25 nm in the 1 % w/v sample to around 80 nm in the 10 % w/v sample. This is consistent with the observation by SEM that the size of the fibrils stays approximately constant but with increased bunching at higher concentrations of gelator. The average pore size is slightly larger in the series templated by **1**, ranging between 19-36 nm, and there is a much broader pore size distribution pattern (Figure S11). The 1 % w/v data sample ranges in pore size up to 80 nm increasing to 120 nm for the 10 % w/v sample. This greater range in pore diameters reflects the broad range of ribbon widths observed by SEM. The shape of the distribution for 5 % w/v **1** is poorly defined and with lower pore volume than for the samples formed with both higher and lower concentrations of gelator. The average pore sizes calculated for both series are generally smaller than might be expected from the SEM images. This is attributed to the presence of macroporisty which is readily observed by SEM but is not taken into account by the BJH model.

Conclusions

By making small changes to the molecular structure of the gelator, and hence to gel morphology, polymeric materials with very different pore shapes, sizes and adsorption characteristics can be created. The entangled networks of cylindrical fibres observed in xerogels of **2** produce polymers with corresponding circular pores and fibrous imprints. Gas adsorption measurements are indicative of a mesoporous material with a random pore structure. The pores formed by **2** have a relatively well defined average pore diameter of 8-9 nm and the total volume increases linearly with the concentration of gelator. In contrast the larger ribbon-like xerogels of **1** give polymers with slit shaped pores and a gas adsorption profile indicative of plate-like aggregates. The average pore diameter is larger and there is a broader pore size distribution reflecting the variable width of the ribbons of **1**. Supramolecular gels provide a ready means of creating porous polymers with very different architectures and properties which can be tuned by varying the concentration and structure of template.

Experimental Section

Reagents and Instruments

All solvents and reagents were obtained from standard commercial sources. Gelators **1** and **2** were prepared according to previously reported protocols.[31] The drying pistol was evacuated using an aspirator and heated by toluene under reflux. All NMR spectra were performed on a Varian DD-700 (700 MHz for ^{1}H, 176 MHz for ^{13}C) and were referenced to residual solvent. Mass spectroscopy was undertaken using a Thermo-Finnigan LTQ FT machine running in positive electron spray (ES) mode. Elemental analysis was performed using an Exeter Analytical Inc. CE-400 Elemental Analyser.

Preparation of polymers

Method 1

0, 5, 25, 50 and 100 mgs of gelators **1** and **2** were weighed into separate 2 ml screw top glass vials. 0.5 ml of a 1:1 by weight methylmethacrylate (MMA): ethylene glycol dimethacrylate (EGDMA) stock solution was added to each vial. The sealed sample was heated until the gelator was fully dissolved and gelation took place rapidly upon cooling. 0.05 ml of a 1:1 MMA:EGDMA solution containing 5 mg (1 % w/v) of 1,1'-azobis(cyclohexane carbonitrile) was layered on top of the sample and allowed to diffuse overnight. The samples were irradiated with 254 nm UV radiation using a UVGL-58 handheld UV lamp for 48 hours at a distance of 5 cm. The samples were washed with hot methanol in a soxhlet for 36 hours. The samples were dried overnight under vacuum in a desiccator. CHN analysis of the polymers showed no nitrogen was present in the polymers indicating removal of the gelator.

Method 2

0, 10, 20, 100 and 200 mgs of gelators 1 and 2 were weighed into separate 10 screw top glass vials. To each vial was added 2 ml of a 1:1 by weight MMA:EGDMA stock solution containing 1 % w/v blend of diphenyl(2, 4, 6-trimethylbenzyl)phosphine oxide and 2-hydroxy-2-methylpropiophenone. The sealed sample was heated until the gelator was fully dissolved then rapidly cooled and sonicated to ensure homogeneous gel formation. The samples were irradiated with 254 nm UV radiation using a UVGL-58 handheld UV lamp for 48 hours at a distance of 5 cm. The samples were washed with hot methanol in a Soxhlet extractor for at least 72 hours. The samples were dried overnight under vacuum in a desiccator. CHN analysis of the polymers showed no nitrogen was present in the polymers indicating removal of the gelator. Suspension of samples of the polymer in d_6-DMSO showed no indication of gelator by NMR spectroscopy.

Scanning electron microscopy

Samples were applied directly to silicon wafer chips (Agar Scientific) using a cocktail stick for gels or a pipette for liquids. Solid samples of polymer were prepared by shattering the brittle polymers and attaching the fragments to the wafers using carbon conductive adhesive tape. Samples were stored under vacuum at $1x10^{-5}$ mbar then sputter coated with 5nm platinum in a Cressington 328 coating unit, at 40 mA (density 21.09 and tooling set at 1) with rotation and a 300 angle of tilt. Samples were imaged using a Hitachi S-5200 field emission scanning electron

microscope at 1.5 kV.

Gas pycnometry

The sample density was measured using an AccuPyc II Micromeitics He pycnometer. The material was then weighed (0.8-1.5 g) into the sample cup (10 cm^3) and placed in the instrument. The sample was then allowed to reach thermal equilibrium with the instrument for 5 to 10 min. The material was then purged 20 times (He(g), 19.5000 psig). The material was then placed under pressure (He(g), 19.5000 psig) and the volume measurements taken once an equilibrium pressure was reached (0.0050 psi min^{-1}). The final density measurement is taken as an average of the 20 repeats and reported with a standard deviation.

Gas adsorption isotherms

The sample was added to a sample tube (1 inch diameter) and then degassed on the instrument (20°C) until a constant pressure was reached. The sample was then weighed (0.8-1.5 g) into the sample tube which was then fitted with a filler rod and isothermal jacket. Nitrogen sorption was then measured under isothermal conditions (77 K) between P/P^0 of 0.0500 to 0.9990 and desorption between 0.999 and 0.140.

BET and Langmuir plots were obtained from measurements at 0.050< P/P0 <0.2500; BJH adsorption and desorption plots were obtained at 0.1400< P/P^0 <0.990. Pore size distributions were obtained using the Faas modified BJH model with a Halsey thickness curve used for the 2 series and the Harkins Jura thickness curve used for the 1 series.

Acknowledgements

We thank the Engineering and Physical Sciences Research Council for Funding.

Notes and references

[a] Department of Chemistry, Durham University, South Road, Durham DH1 3LE, UK. E-mail: jon.steed@durham.ac.uk; Tel: +44 (0)191 334 2085

† Electronic Supplementary Information (ESI) available: Additional SEM images and gas adsorption isotherms provided. See DOI: 10.1039/b000000x/

1. P. Terech and R. G. Weiss, *Chem. Rev.*, 1997, **97**, 3133-3160.
2. J. W. Steed, *Chem. Commun.*, 2011, **47**, 1379-1383.
3. A. R. Hirst, B. Escuder, J. F. Miravet and D. K. Smith, *Angew. Chem., Int. Ed.*, 2008, **47**, 8002–8018.
4. M. Llusar and C. Sanchez, *Chem. Mat.*, 2008, **20**, 782-820.
5. A. M. Seddon, H. M. Patel, S. L. Burkett and S. Mann, *Angew. Chem. Int. Ed.*, 2002, **41**, 2988-2991.
6. J. L. Zhou, X. J. Chen and Y. S. Zheng, *Chem. Commun.*, 2007, 5200-5202.
7. N. M. Sangeetha and U. Maitra, *Chem. Soc. Rev.*, 2005, **34**, 821-836.
8. X. Yang, G. Zhang and D. Zhang, *J. Mater. Chem.*, 2012, **22**, 38-50.
9. K. J. C. van Bommel, A. Friggeri and S. Shinkai, *Angew. Chem., Int. Ed.*, 2003, **42**, 980-999.
10. M.-O. M. Piepenbrock, N. Clarke, J. A. Foster and J. W. Steed, *Chem. Commun.*, 2011, **47**, 2095-2097.
11. J. D. Hartgerink, E. Beniash and S. I. Stupp, *Science*, 2001, **294**, 1684-1688.
12. F. Ouhib, E. Bugnet, A. Nossov, J.-L. Bonardet and L. Bouteiller, *Polymer*, 2010, **51**, 3360-3364.
13. S. Srinivasan, P. A. Babu, S. Mahesh and A. Ajayaghosh, *J. Am. Chem. Soc.*, 2009, **131**, 15122-15123.
14. J. C. Stendahl, E. R. Zubarev, M. S. Arnold, M. C. Hersam, H. J. Sue and S. I. Stupp, *Adv. Funct. Mater.*, 2005, **15**, 487-493.
15. D. A. Stone, L. Hsu, N. R. Wheeler, E. Wilusz, W. Zukas, G. E. Wnek and L. T. J. Korley, *Soft Matter*, 2011, **7**, 2449-2455.
16. J. R. Moffat and D. K. Smith, *Chem. Commun.*, 2011, **47**, 11864-11866.
17. E. R. Zubarev, M. U. Pralle, E. D. Sone and S. I. Stupp, *Adv. Mater.*, 2002, **14**, 198-203.
18. G. Tan, M. Singh, J. He, V. T. John and G. L. McPherson, *Langmuir*, 2005, **21**, 9322-9326.
19. M. I. Burguete, F. Galindo, R. Gavara, M. A. Izquierdo, J. C. Lima, S. V. Luis, A. J. Parola and F. Pina, *Langmuir*, 2008, **24**, 9795-9803.
20. J. R. Moffat, G. J. Seeley, J. T. Carter, A. Burgess and D. K. Smith, *Chem. Commun.*, 2008, 4601-4603.
21. F.-X. Simon, N. S. Khelfallah, M. Schmutz, N. Díaz and P. J. Mésini, *J. Am. Chem. Soc.*, 2007, **129**, 3788-3789.
22. U. Beginn, S. Sheiko and M. Möller, *Macromol. Chem. Phys.*, 2000, **201**, 1008-1015.
23. W. Q. Gu, L. D. Lu, G. B. Chapman and R. G. Weiss, *Chem. Commun.*, 1997, 543-544.
24. R. J. H. Hafkamp, B. P. A. Kokke, I. M. Danke, H. P. M. Geurts, A. E. Rowan, M. C. Feiters and R. J. M. Nolte, *Chem. Commun.*, 1997, 545-546.
25. Q. Wei and S. L. James, *Chem. Commun.*, 2005, 1555-1556.
26. D. Wu, F. Xu, B. Sun, R. Fu, H. He and K. Matyjaszewski, *Chem. Rev.*, 2012, **112**, 3959-4015.
27. H.-S. Yun, J.-W. Park, S.-H. Kim, Y.-J. Kim and J.-H. Jang, *Acta Biomaterialia*, 2011, **7**, 2651-2660.
28. W. Xuan, C. Zhu, Y. Liu and Y. Cui, *Chem. Soc. Rev.*, 2012, **41**, 1677-1695.
29. Z. Li, J. C. Barnes, A. Bosoy, J. F. Stoddart and J. I. Zink, *Chem. Soc. Rev.*, 2012, **41**, 2590-2605.
30. J. A. Foster, M.-O. M. Piepenbrock, G. O. Lloyd, N. Clarke, J. A. K. Howard and J. W. Steed, *Nature Chem.*, 2010, **2**, 1037-1043.
31. J. A. Foster, R. M. Edkins, G. J. Cameron, N. Colgin, K. Fucke, S. Ridgeway, A. G. Crawford, T. B. Marder, A. Beeby, S. L. Cobb and J. W. Steed, *Chem. Eur. J.*, 2013, DOI: 10.1002/chem.201303153.
32. G. E. Keck and D. A. Burnett, *J. Org. Chem.*, 1987, **52**, 2958-2960.
33. D. K. Smith, *Chem. Soc. Rev.*, 2009, **38**, 684-694.
34. M. de Loos, J. van Esch, R. M. Kellogg and B. L. Feringa, *Angew. Chem., Int. Ed.*, 2001, **40**, 613-616.
35. R. K. Das, R. Kandanelli, J. Linnanto, K. Bose and U. Maitra, *Langmuir*, 2010, **26**, 16141-16149.
36. S. Yoshizawa, T. Utsugi, K. Shibano, S. Goto and H. Yajima, *Trans. Mater. Res. Soc. Jpn.*, 2005, **30**, 1155-1158.
37. Z. Shan, T. Maschmeyer, J. C. Jansen, *US Pat.*, US 6814950, 2004.
38. F. Audouin, M. Birot, E. Pasquinet, O. Besnard, P. Palmas, D. Poullain and H. Deleuze, *Macromolecules*, 2011, **44**, 4879-4886.
39. K. S. W. Sing, D. H. Everett, R. A. W. Haul, L. Moscou, R. A. Pierotti, J. Rouquerol and T. Siemieniewska, *Pure and Applied Chemistry*, 1985, **57**, 603-619.
40. S. Lowell, J. E. Shields, M. A. Thomas and M. Thommes, *Characterization of Porous Solids and Powders: Surface Area, Pore Size and Density*, Springer, The Netherlands, 2006.

Graphical Abstract

Polymerisation of methyl methacrylate supramolecular gels followed by removal of the gelator imprints the gel morphology into the covalent polymer.